

**Subsea Pipelines Health Prognostics Using Rate of Crack
Propagation and Marco-Starkey, Cumulative Damage
Theory**

BY

MOHAMED FAZLAN BIN NIZAMUDDIN

16370

Progress report submitted in partial fulfillment of
the requirements for the Degree of Study(Hons)
(Mechanical)

Final Year Project II January 2016

Universiti Teknologi PETRONAS
Bandar Seri Iskandar
31750 Tronoh
Perak Darul Ridzuan

CERTIFICATION OF APPROVAL

**Subsea Pipelines Health Prognostics Using Rate of Crack
Propagation and Marco-Starkey, Cumulative Damage
Theory**

by

Mohamed Fazlan bin Nizamuddin

16370

A project dissertation submitted to the
Mechanical Engineering Programme
Universiti Teknologi PETRONAS
in partial fulfilment of the requirement for the
BACHELOR OF ENGINEERING (Hons)
(Mechanical)

Approved by,

(Name of Main Supervisor)

UNIVERSITI TEKNOLOGI PETRONAS

TRONOH, PERAK

January 2006

CERTIFICATION OF ORIGINALITY

This is to certify that I am responsible for the work submitted in this project, that the original work is my own except as specified in the references and acknowledgements, and that the original work contained herein have not been undertaken or done by unspecified sources or persons.

MOHAMED FAZLAN BIN NIZAMUDDIN

ABSTRACT

The prevention of failure in subsea pipelines has been a priority of users in many fields. Through prognosis, the Remaining useful life (RUL) of pipes can be predicted, and with proper maintenance techniques, its RUL can be extended. Subsea pipelines may experience fatigue failure due to cracks initiated as result of corrosion and cyclic stress. Hence, there is a need for estimating remaining useful life once the crack is detected. To ensure this, a proper prognostic will be developed predicting the RUL of these pipelines. A generic MATLAB framework will be developed to ensure easy prognostics of the pipelines. This framework will investigate the effects of crack orientation and magnitude of stress on the RUL. It will also investigate the effect of uncertainty in the initial crack estimation to RUL prediction. The whole process would be accomplished first by studying the literature regarding crack propagation. Once the basic concepts are grasped, studies have to be done on the geometry of different types of cracks. Once the model is selected it is simulated and the RUL can be estimated. It can be seen that the trend of crack propagation is the same regardless of magnitude of stress used however the number of cycles until it reaches failure is the key point to look at. The higher the stress used the faster the pipe would reach failure. Also, different cracks propagate at different rates depending on the stress intensity factor. This project can be further expanded by studying the effect of non-linear damage propagation models. Also, the average pressure in pipelines can be taken into consideration when calculating the rate of crack propagation.

CONTENTS

ABSTRACT	iii
CONTENTS	iv
LIST OF FIGURES	vi
LIST OF TABLES	viii
NOMENCLATURE AND ABBREVIATIONS	ix
CHAPTER 1 : INTRODUCTION	1
1.1 Background of Study	1
1.2 Problem Statement	2
1.3 Objectives	3
1.4 Scope of study	3
CHAPTER 2 : LITERATURE REVIEW	4
2.1 Introduction	4
2.2 Rate of Crack Propagation	7
2.3 Stress Intensity Factor	10
2.4 Stress equation for thin walled and thick walled pipes	16
2.5 Wohler’s Curve	17
2.6 Estimating Remaining Useful Life	18
2.7 Summary	19
CHAPTER 3 : METHODOLOGY	21
3.1 Introduction	21
3.1.1 Literature Review	21
3.1.2 Fundamental equation and crack propagation/model	22
3.1.3 MATLAB modeling and computation	22
3.1.4 Parametric Study and Regression Analysis	22
3.1.5 Further Analysis and Report Writing	22

3.2 Solution Method	25
CHAPTER 4 : RESULTS	26
4.1 Introduction	26
4.2 MATLAB Modeling	26
4.2.1 Investigation of the relationship of RUL with varying magnitudes of internal pressure using longitudinal crack	26
4.2.2 Investigation of the relationship of RUL by taking into account uncertainties in subsea pipelines	29
4.2.3 Investigation of the relationship of RUL with varying magnitudes of internal pressure using circumferential crack	30
4.2.4 Investigation of the relationship of RUL with varying magnitudes of internal pressure using semi-elliptical crack ...	32
4.2.5 Comparing the relationship of RUL with varying types of cracks	33
4.3 Discussion	34
CHAPTER 5 : CONCLUSION AND RECOMMENDATION	36
5.1 Conclusion	36
5.2 Recommendation	36
REFERENCES	37
APPENDIX-A	39

LIST OF FIGURES

Figure 1.1: Examples of offshore structures. [2]	2
Figure 2.1: Fracture Modes a) Mode I (Opening) b) Mode II (Sliding) c) Mode III Tearing) [4].....	4
Figure 2.2: Linear Damage Accumulation [5].....	5
Figure 2.3: Non-linear Damage Law [5].....	5
Figure 2.4: Marco-Starkey, cumulative damage theory [5]	6
Figure 2.5: Pre-crack fatigue damage [6].....	7
Figure 2.6: Crack length evolution [6].....	7
Figure 2.7: Stages in Fatigue Life.....	8
Figure 2.8: The three stages of crack growth according to Paris-Erdogans law [6].....	8
Figure 2.9: Boundary correction factor for semi-circular crack in an internally pressurized cylinder [12]	12
Figure 2.10: Boundary correction factor for semi-elliptical crack in an internally pressurized cylinder. [12]	12
Figure 2.11: Circumferential crack in a cylindrical shell.....	13
Figure 2.12: Longitudinal crack in a cylindrical shell	14
Figure 2.13: Elliptical crack in a thick-walled cylinder[13].....	15
Figure 2.14: Stress distribution along a pipe. [14].....	16
Figure 2.15: Graph of cyclic stress [6].....	17
Figure 2.16: Wohler's curve of fatigue [6]	18
Figure 2.17: Stresses experienced by a pipe underwater[6].....	19
Figure 3.1: Methodology Flow Chart.....	21
Figure 3.2: Project Flow Chart	23
Figure 3.3 a) Gantt chart FYP I (b) Gant chart FYP II (c) Key Milestones	24
Figure 4.1: Stresses in a subsea pipeline	27

Figure 4.2: (a) Graph of crack length against cycles for longitudinal crack (b) Graph of damage against cycles for longitudinal crack.....	28
Figure 4.3: Graph of probability against crack length	30
Figure 4.4: (a) Graph of crack length against cycles for circumferential crack (b) Graph of damage against cycles for circumferential crack.....	31
Figure 4.5: (a) Graph of crack length against cycles for Semi-elliptical crack (b) Graph of damage against cycles for Semi-elliptical crack.....	33
Figure 4.6: Comparison of 3 graphs.....	34

LIST OF TABLES

Table 2-1: Description of fracture modes.....	4
Table 2-2: Crack growth rate coefficients for various drill pipe materials[9]	10

NOMENCLATURE AND ABBREVIATIONS

RUL	Remaining useful lifetime
e, t	Wall thickness
a_o	Initial crack length
a_c	Critical crack length
N	Cycle number
N_c	Critical cycle
C, m	Environmental parameters for crack growth
K_I	Stress intensity factor for mode I
ΔK	Change in stress intensity factor
K_c	Critical stress intensity factor
K_{th}	Stress intensity factor threshold
σ	Stress exerted in the pipe
$Y(a), F(\lambda)$	Geometric factor function of the pipeline geometric features
Q	Shape factor for elliptical crack
G_j	Boundary-correction factor
F	Boundary correction factor for internally pressurized cylinder
a	Crack depth for elliptical and circular crack
c	Crack length for elliptical and circular crack
R	Radius of cylinder
σ_h	Hoop stress
σ_a	Axial stress

σ_r

Radial stress

CHAPTER 1 : INTRODUCTION

1.1 Background of Study

Fatigue failure represents a failure that occurs due to repeated loads applied upon a certain area. Due to these loads, the material progressively becomes weaker and weaker until failure occurs. This cyclic loading would result in a stress value that's less than the ultimate tensile stress limit or yield stress limit to damage the material. Tiny cracks will begin to form on the surfaces where the stress concentrators are. In time, each crack would propagate until one reaches its critical size causing the material to fail. Pipelines are designed circular because the round surface distributes the stresses equally along the surface. Generally, shapes with sharp holes or sharp corners experience elevated stresses inviting fatigue cracks to occur.

When testing fatigue failure, load has to be applied gradually as to ensure the specimen has sufficient time for the strain to develop in it. These specimens will be tested to failure meaning each specimen can only run the test once. To simulate best results, specimens are tested in conditions approximately as close as possible to actual conditions many structural and machine members would be subjected to.

Fatigue Failure can be said to be more dangerous as compared to static failure. In most cases, static failure would be able to be seen visibly for example, abnormally large deflection in a certain part. This could easily be rectified by simply replacing the part brand new. Fatigue failure however, leaves no apparent traces before occurring. It is very unpredictable and visually undetectable making it very dangerous in any line of engineering. Fatigue failure is still a relatively unknown field and therefore hard to fully prevent.

The concept of prognosis started off in the field of medicine whereby the olden Greek physician Hippocrates [1] stated , “It appears to me a most excellent thing for the physician to cultivate Prognosis; for by foreseeing and foretelling, in the presence of the sick, the present, the past, and the future, and explaining the omissions which patients have been guilty of, he will be the more readily believed to be acquainted with the circumstances of the sick; so that men will have confidence to entrust themselves to such a physician.” In time, the prognosis field moved on to not just estimating the remaining life, but rather finding a cure to extend the life. With the term prognosis becoming more and more popular, the field of study for

Besides that, the linear version of damage accumulation law overlooks the random stress sequence and prognostics based on nonlinear version. The non-linear version has not been applied to subsea pipelines.

1.3 Objectives

By conducting this project, a couple of objectives have to be achieved:

- To develop a prognostic or Remaining Useful Life (RUL) prediction model for subsea pipelines based on crack propagation and nonlinear damage accumulation models.
- To develop a generic and MATLAB based framework for easy analysis of prognostics in subsea pipelines
- To investigate the effect of uncertainty in the initial crack estimation to RUL prediction
- To investigate the effect of crack orientation and stress magnitude to RUL.

1.4 Scope of study

Throughout the study for this project, we would have to study in depth regarding the relationship between crack propagation and fatigue lifetime in pipelines when subjected to cyclic loading. Many different aspects will be looked into in order to calculate the rate of propagation of cracks. These aspects will be the following:

- Pipe Geometry and location
 - Thin, thick walled pipes. Shallow, deep or ultra-deep water depth.
- Crack geometry and location
 - Internal, thumbnail, external, circumferential
- Failure Mode
 - Mode I, Mode II, Mode III
- Analysis Option
 - Deterministic, Stochastic

CHAPTER 2 : LITERATURE REVIEW

2.1 Introduction

In the past, there have been studies on the prognosis of the subsea pipelines through various methods. Vaidya [3], has talked about an overall tool for the prognosis of subsea oil and gas industry. Using the Bayesian Belief Network, many conditions have to be taken into account such as the technical condition, operational history, design quality, as well as the future operating conditions and future environment conditions. Taking all these into account, will be able to calculate the probability of the posterior occurring whereby:

$$Posterior = \frac{Prior \times Likelihood}{Normalizing Constant} \quad (1)$$

Out of the any types of crack, each crack can only undergo 3 types of independent movement which would result in 3 fundamental fracture modes. These modes are called Mode I, Mode II and Mode III. Fractures are always described in one of these 3 modes or a combination.

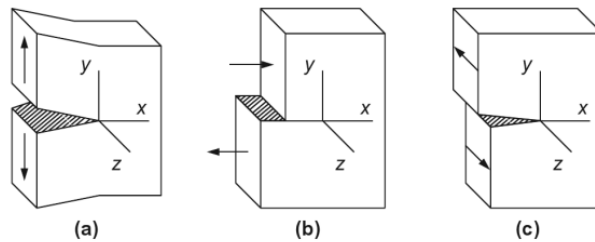


Figure 2.1: Fracture Modes a) Mode I (Opening) b) Mode II (Sliding) c) Mode III Tearing) [4]

Table 2-1: Description of fracture modes

Mode	Description
Mode I	The opening mode occurs when the two cracked surfaces experience a jump in the u_y direction. It would result in an undeformed crack-plane in the xz -plane.
Mode II	The Sliding mode occurs when the two cracked surfaces experience a jump in the u_x direction. It would result in an undeformed crack-plane in the yz -plane when they slide against each other.
Mode III	The Tearing mode occurs when the two cracked surfaces experience a jump in the u_z direction. It would result in an undeformed crack-plane in the yz -plane.

Going into other prognostic models, El-Tawil & Jaoude[5] has done a study on the stochastic and non-linear based prognostic model. Using the damage accumulation law and Palmgren-Miner linear rule, 2 figures were given.

For the Linear damage accumulation, we can see that for a lower initial stress, ϵ_1 a slower damage accumulation occurs and when the higher stress, ϵ_2 is applied, the damage accumulation increases tremendously. The vice versa can be said when a higher initial stress is applied followed by a smaller stress.

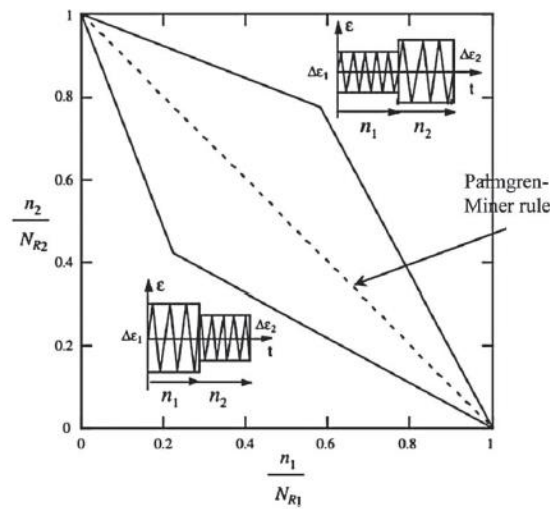


Figure 2.2: Linear Damage Accumulation [5]

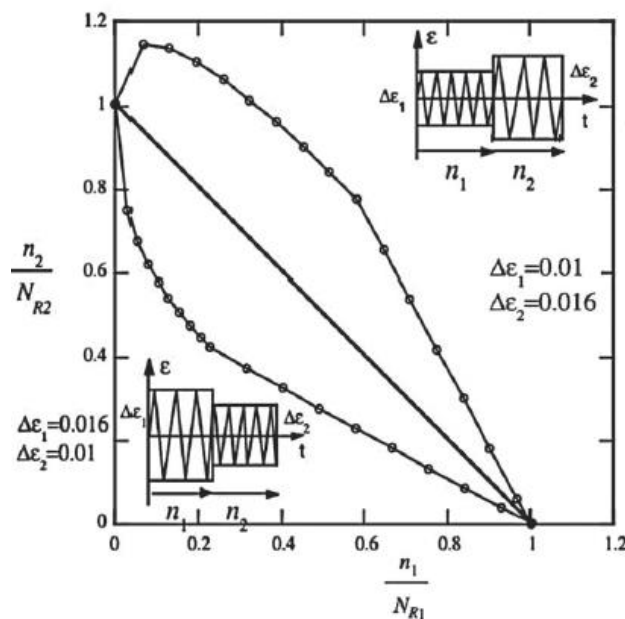


Figure 2.3: Non-linear Damage Law [5]

The Marco-Starkey, cumulative damage theory for cyclic stresses is also discussed in the journal. This damage accumulation theory explains on different magnitudes of cyclic stresses and how their rate of damage accumulation slowly increases over time. The test with a lower cyclic stress degrades at a much slower rate as compared to the higher cyclic stress.

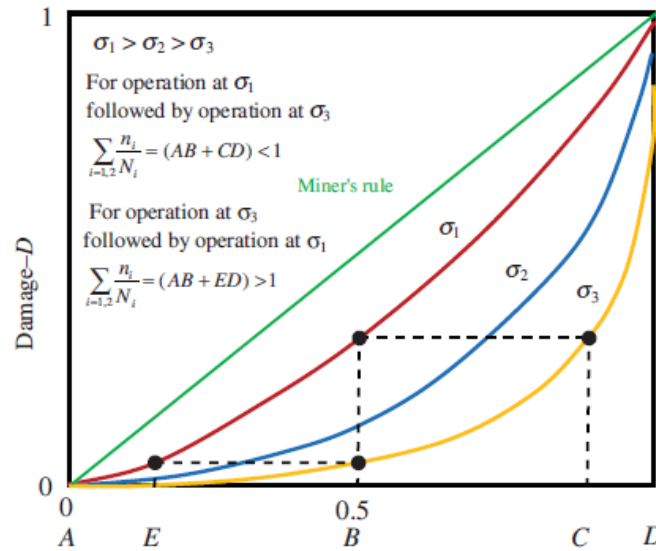


Figure 2.4: Marco-Starkey, cumulative damage theory [5]

In 2013, Abou Jaoude[6] also released a Thesis on the study of prognostics in subsea pipelines. This thesis studies very deeply on more types of prognostic models both linear and non-linear.

The Damage Evolution Law states that materials going under cyclic loading will incur micro-cracks. Once the cyclic loading reaches a cycle of N_0 , the crack length, a_0 becomes detectable and unstable. As the cycle keeps increasing until the cycle N_c the crack length increases as well until the crack length reaches a critical length, a_c and fails. The critical length, $a_c = e/8$ where e is the device dimension in the crack direction. l Would be the length perpendicular to the crack direction and t_N corresponds to the instantaneous time at a cycle N .

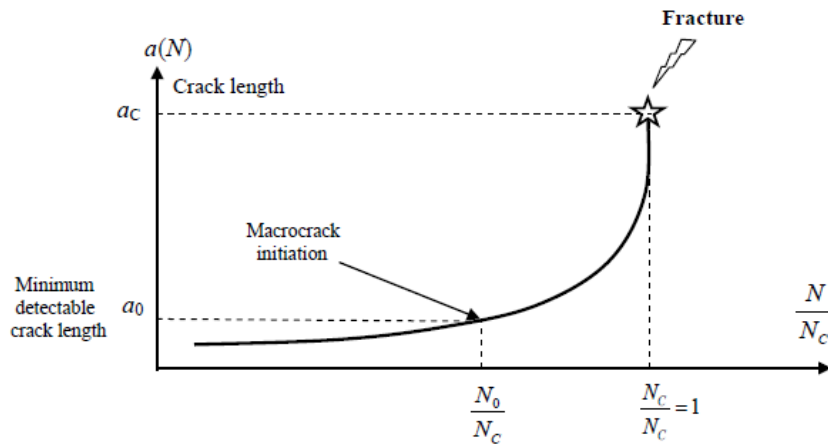


Figure 2.5: Pre-crack fatigue damage [6]

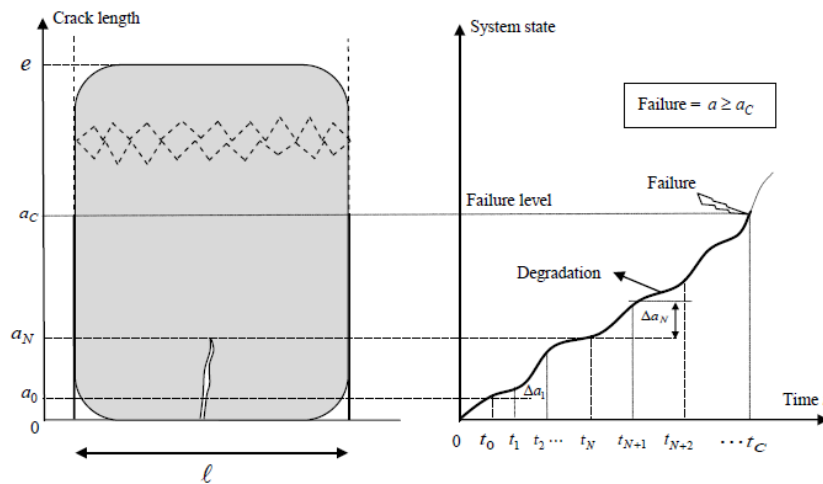


Figure 2.6: Crack length evolution [6]

2.2 Rate of Crack Propagation

In the past many models for rate of crack propagation have been formulated taking into account both constant and variable amplitude loadings. In the early 1950's, investigators stated that microcracks can be observed even in the early stages of the fatigue life[7]. A conclusion was drawn stating that fatigue life under cyclic stress, can be broken down into two stages namely the crack initiation stage, and the crack propagation stage. The entire process can be seen in figure 2.7.



Figure 2.7: Stages in Fatigue Life

Another prognostic model would be the Paris-Erdogan law. This law relates the stress intensity factor with the rate of propagation of the crack. The formula used would be

$$\frac{da}{dN} = C\Delta K^m \quad (2)$$

Where da/dN signifies the rate of crack growth with respect to number of cycles. C and m are the environmental parameters and K is the stress intensity factor. ΔK denotes the difference of the maximum stress intensity factor and the minimum stress intensity factor to open the fatigue crack.

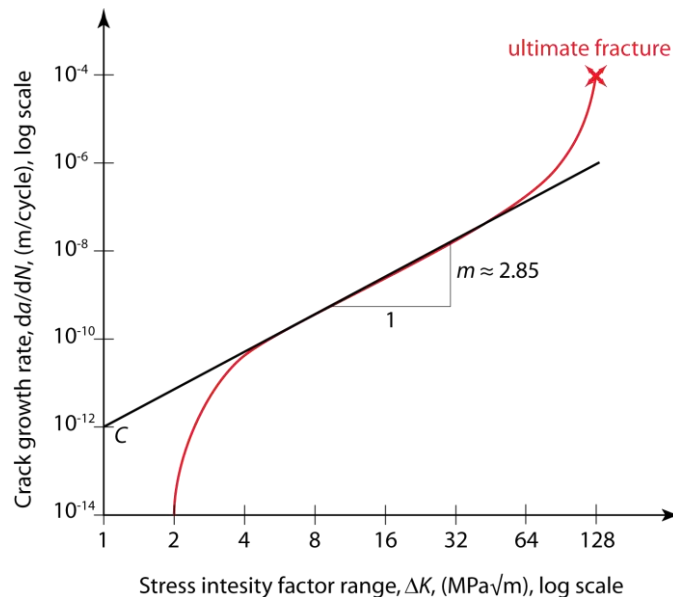


Figure 2.8: The three stages of crack growth according to Paris-Erdogans law [6]

However, the Paris-Erdogan law does have a weakness which is it does not take into account the stress ratio and is also dependant on the material used. Besides that, it is only accurate when the length of the plastic zone ahead of the crack tip is long compared to with the mean grain size but much smaller in crack length.

Many different models have been formulated by other researchers to further extend the applications on crack propagation prediction. Some of these models are:

i) Collipriest Model [8]:

$$\frac{da}{dN} = C(K_c \Delta K)^{m/2} EXP \left[\ln \left(\frac{K_c}{\Delta K_o} \right) \tanh^{-1} \left(\frac{\ln \left(\frac{\Delta K^2}{(1-R)K_c K_o} \right)}{\ln \left(\frac{(1-R)K_c}{\Delta K_o} \right)} \right) \right] \quad (3)$$

ii) McEvily Model [8]:

$$\frac{da}{dN} = \frac{4A}{\pi \sigma_y E} (\Delta K^2 - \Delta K_{th}^2) \quad (4)$$

iii) Frost and Pook Model [8]:

a) For plain stress:

$$\frac{da}{dN} = \frac{9}{\pi} \left(\frac{\Delta K^2}{E} \right) \quad (5)$$

b) For plain strain:

$$\frac{da}{dN} = \frac{7}{\pi} \left(\frac{\Delta K^2}{E} \right) \quad (6)$$

Various studies have been done in order to study the geometric or environmental properties for the Paris-Erdogan Law. A list of values for C and m and be obtained from Table 2-2, for common drill pipe materials.

Table 2-2: Crack growth rate coefficients for various drill pipe materials[9]

Type of Material	Environmental Parameter, <i>C</i>	Environmental Parameter, <i>m</i>
API grade E	$4.41 * 10^{-10}$	2.94
API grade X	$9.35 * 10^{-10}$	2.65
API grade G	$1.60 * 10^{-9}$	2.52
API grade S	$1.60 * 10^{-9}$	2.52
4145 MOD Steel(box)	$1.152 * 10^{-9}$	2.68
4145 MOD Steel(pin)	$3.083 * 10^{-10}$	3.07

2.3 Stress Intensity Factor

An important parameter in the Paris-Erdogan's law will be the stress intensity factor, K . The stress intensity factor [10] is a parameter that amplifies the magnitude of applied stress. The stress intensity factor is calculated separately for each mode. Fracture will only take place when one of the stress intensity factors, K_I , K_{II} or K_{III} , reaches its corresponding critical value, K_{Ic} , K_{IIc} or K_{IIIc} [11]. The critical stress intensity factor for each material is always constant. The stress intensity factor when considering a flat crack in the system body can be expressed as:

$$K_I^m = (Y(a) \cdot \sqrt{\pi a})^m \sigma_{max}^m \quad (7)$$

Where,

$$Y(a) = 0.6 * \frac{1 + 2\left(\frac{a}{e}\right)}{\left(1 - \frac{a}{e}\right)^{3/2}} \quad (8)$$

However, flat cracks are not the only type of cracks that occur. It is important to identify which type of crack is present in the system. Thorough research using three-dimensional finite element method has been done in order to identify the stress intensity factor for both semi-circular and semi elliptical crack shapes for Mode I type cracks. The equation [12] is as follows:

$$K_I = \sqrt{\pi \frac{a}{Q}} G_j \left(\frac{a}{c}, \frac{a}{t}, \frac{R}{t}, \phi \right) \quad (9)$$

Where, G_j is a boundary-correction factor corresponding the j^{th} stress distribution. This stress distribution are calculated using the formula

$$\sigma_j = \left(\frac{z}{a} \right)^j \quad (10)$$

Where $j=0$ to 3. The Q value however is the shape factor for elliptical crack, calculated using the formula

$$Q = 1 + 1.464 \left(\frac{a}{c} \right)^{1.65} \quad (11)$$

When the cylinder is pressurized, a slightly different stress intensity factor formula[12] was obtained.

$$K_I = \frac{pR}{t} \sqrt{\pi \frac{a}{Q}} F \left(\frac{a}{c}, \frac{a}{t}, \frac{R}{t}, \phi \right) \quad (12)$$

Where, F is the boundary correction factor for the inside of an internally pressurized cylinder. F has been determined in terms of G_j using the first four terms of a power series expansion of Lamé's Solution[12]:

$$F = \frac{t}{R} \left(\frac{R_o^2}{R_o^2 - R^2} \right) * \left[2G_0 - 2 \left(\frac{a}{R} \right) G_1 + 3 \left(\frac{a}{R} \right)^2 G_2 - 4 \left(\frac{a}{R} \right)^3 G_3 \right] \quad (13)$$

The Results of F was computed for both a semi-circular crack and semi elliptical crack. Two ratios of $\frac{a}{t}$ (0.8 & 0.2) were used and tested with varying $\frac{t}{R}$ ratios (0, 0.1 & 0.25). These values can be seen from Figure 2.9 and Figure 2.10 as below.

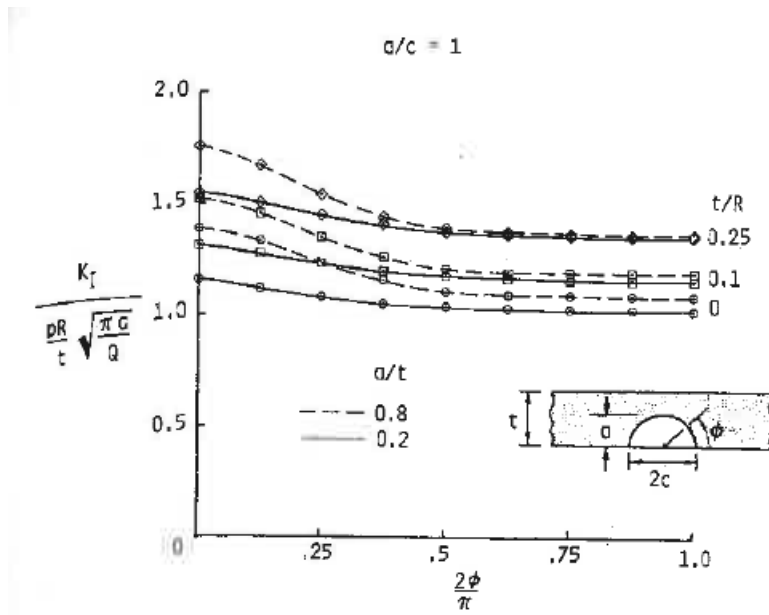


Figure 2.9: Boundary correction factor for semi-circular crack in an internally pressurized cylinder [12]

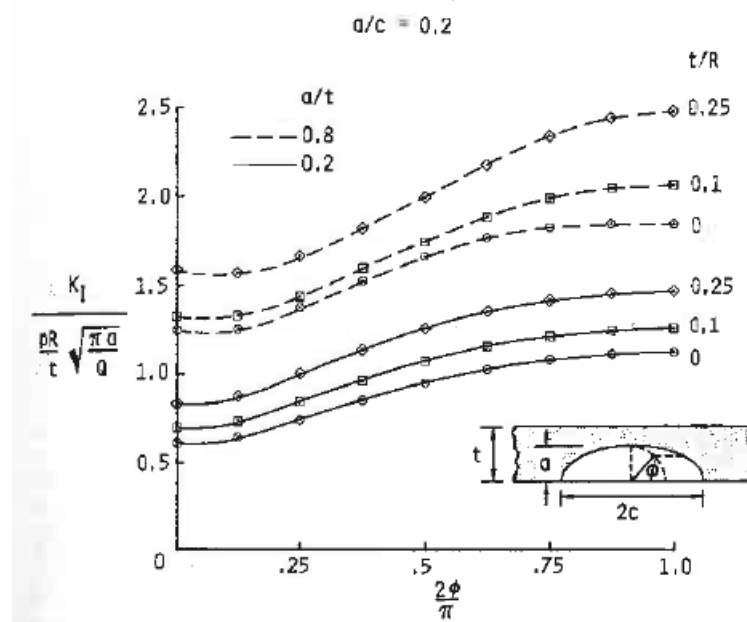


Figure 2.10: Boundary correction factor for semi-elliptical crack in an internally pressurized cylinder. [12]

Another approach can be used[12] in order to calculate the stress intensity factor in which:

$$F = 0.97 \left[M_1 + M_2 \left(\frac{a}{t} \right)^2 + M_3 \left(\frac{a}{t} \right)^4 \right] g f_{\phi} f_c \quad (14)$$

Where,

$$M_1 = 1.13 - 0.09 \frac{a}{c} \quad (15)$$

$$M_2 = -0.54 + \frac{0.89}{0.2 + \frac{a}{c}} \quad (16)$$

$$M_3 = 0.5 - \frac{1}{0.65 + \frac{a}{c}} + 14 \left(1 - \frac{a}{c} \right)^{24} \quad (17)$$

$$g = 1 + \left[0.1 + 0.35 \left(\frac{a}{t} \right)^2 \right] (1 - \sin \phi)^2 \quad (18)$$

$$f_{\phi} = \left[\sin^2 \phi + \left(\frac{a}{c} \right)^2 \cos^2 \phi \right]^{1/4} \quad (19)$$

$$f_c = \left[\frac{R_o^2 + R^2}{R_o^2 - R^2} + 1 - 0.5 \sqrt{\frac{a}{t}} \right] \frac{t}{R} \quad (20)$$

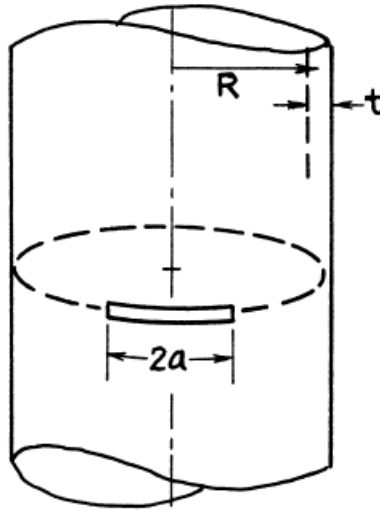


Figure 2.11: Circumferential crack in a cylindrical shell

Another form of crack to look into is the circumferential crack and longitudinal crack in a cylindrical shell. First of all, we look into the circumferential cracks as shown in Figure 2.11. When considering these cracks, we take the axial stress as in Equation (32) to be considered for the stress intensity factor. The formula to calculate the stress intensity factor will be:

$$K_I = \sigma\sqrt{\pi a} * F(\lambda) \quad (21)$$

Where,

$$\lambda = \frac{a}{\sqrt{Rt}} \quad (22)$$

$$F(\lambda) = (1 + 0.3225\lambda^2)^{\frac{1}{2}} \quad 0 < \lambda \leq 1 \quad (23)$$

$$F(\lambda) = 0.9 + 0.25\lambda \quad 1 < \lambda \leq 5 \quad (24)$$

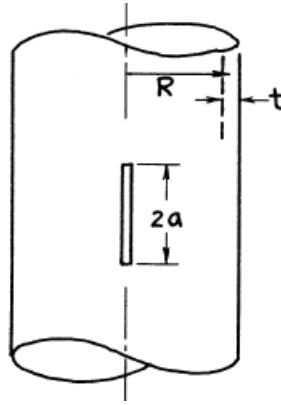


Figure 2.12: Longitudinal crack in a cylindrical shell

Next we consider the longitudinal crack as in Figure 2.12. When evaluating this crack, we use the hoop stress formula as in Equation (31) to be considered in the calculation for stress intensity formula. The same stress intensity formula as in Equation (21) is used but with different parameters such as:

$$F(\lambda) = (1 + 1.25\lambda^2)^{\frac{1}{2}} \quad 0 < \lambda \leq 1 \quad (25)$$

$$F(\lambda) = 0.6 + 0.9\lambda \quad 1 < \lambda \leq 5 \quad (26)$$

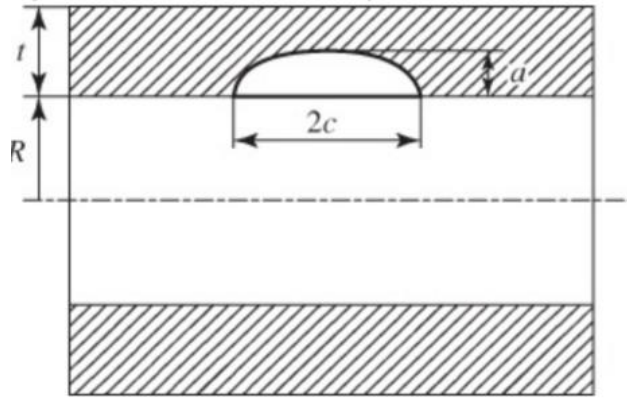


Figure 2.13: Elliptical crack in a thick-walled cylinder[13]

When considering thick-walled cylinders however, the stress intensity factor has to be modelled slightly differently. First of all, the hoop stress experienced by the cylinder will be[13]:

$$\sigma_h = \frac{D_i^2 p_i}{D_o^2 - D_i^2} \left(1 + \frac{D_o^2}{4r^2} \right) \quad (27)$$

The stress intensity factor can be modelled as[13]:

$$K_I = \frac{p_i R}{t} \sqrt{\frac{\pi a}{Q}} F \left(\frac{a}{t}, \frac{a}{2c}, \frac{R}{t} \right) \quad (28)$$

Where,

$$F = 1.12 + 0.053\xi + 0.0053\xi^2 + (1 + 0.02\xi + 0.0191\xi^2) \frac{(20 - R/t)^2}{1400} \quad (29)$$

Where,

$$\xi = \left(\frac{a}{t}\right) \left(\frac{a}{2c}\right) \quad (30)$$

However, this equation is only valid for $5 \leq R/1 \leq 20$, $2c/a \leq 12$ and $a/t \leq 0.80$

2.4 Stress equation for thin walled and thick walled pipes.

When looking at pipelines, it can either be classified as thin walled or thick walled. To classify these two, a thin walled pipe would have a thickness, t of less than $1/20$ of the diameter, D . A pipeline with a thickness larger than this would be classified as a thick walled pipe. The stress can be calculated by either hoop stress, σ_h axial stress, σ_a and by radial stress σ_r . These stress distributions can be explained through Figure 2.14.

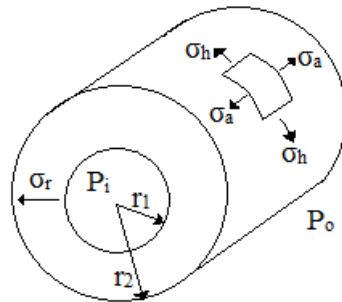


Figure 2.14: Stress distribution along a pipe. [14]

For a thin walled pipe, the stress equations[15] will be as follows.

Hoop Stress:
$$\sigma_h = \frac{Pr}{t} \quad (31)$$

Axial Stress:
$$\sigma_a = \frac{Pr}{2t} \quad (32)$$

Radial Stress:
$$\sigma_r = \frac{-P}{2} \quad (33)$$

For thick walled pipe however, the stress equations will be as follows:

Hoop Stress:
$$\sigma_h = \frac{p_i r_i^2 - p_o r_o^2}{r_o^2 - r_i^2} + \frac{(p_i - p_o) r_o^2 r_i^2}{(r_o^2 - r_i^2) r^2} \quad (34)$$

Axial Stress:
$$\sigma_a = \frac{p_i r_i^2}{r_o^2 - r_i^2} \quad (35)$$

Radial Stress:
$$\sigma_r = \frac{p_i r_i^2 - p_o r_o^2}{r_o^2 - r_i^2} - \frac{(p_i - p_o) r_o^2 r_i^2}{(r_o^2 - r_i^2) r^2} \quad (36)$$

Where, p_i is internal pressure; r_i is internal radius; p_o is external pressure; r_o is external radius; r is radius at the point of interest.

2.5 Wohler's Curve

Wohler's curve expresses the relationship between the applied cyclic stress and the critical cycle associated to the stress. This curve is also known as the S-N curve. To graphically explain the cyclic stress, a sinusoidal graph is plotted.

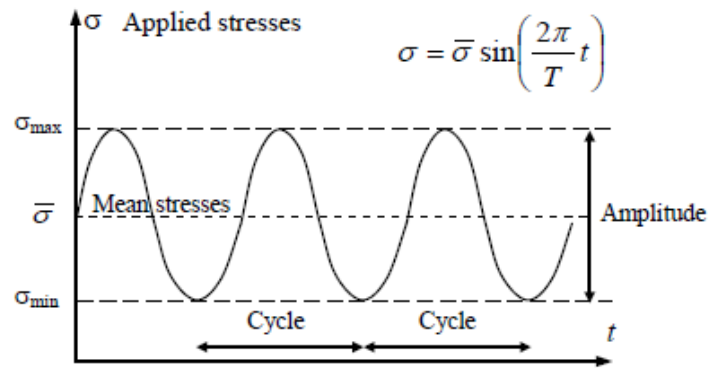


Figure 2.15: Graph of cyclic stress [6]

Once a proper understanding of the stresses is done, the relationship between different stresses and the critical cycle is plotted. It can be said that when a high cyclic stress is tested, the number of cycles the material can undergo will be very little as compared to when a lower cyclic stress exerted.

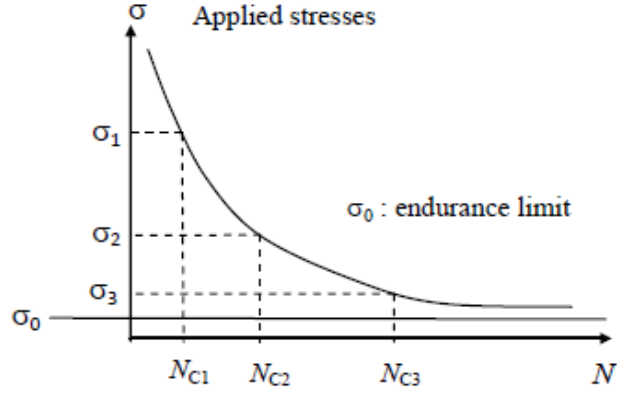


Figure 2.16: Wohler's curve of fatigue [6]

2.6 Estimating Remaining Useful Life

The RUL signifies the amount of time left until the crack length reaches its critical length a_c . In order to determine this parameter, we first calculate the rate of crack growth from the initial crack size of a_o which is modelled as[16]:

$$\frac{da}{dN} = C(\Delta K)^m \left[\frac{1 - (\Delta K_{th}/\Delta K)^{n_1}}{1 - (\Delta K_{max}/K_c)} \right]^{n_3} \quad (37)$$

Where,

K_{th} = Threshold value of stress intensity factor.

The RUL can then be calculated using the expression[16]:

$$t_{rem} = \frac{a_c - a_i}{da/dt} \quad (38)$$

The relation of Equation (37) and Equation (38) can be used when calculating residual life estimation.

2.7 Summary

It is taken into account that there are a lot of factors to consider before carrying out the simulation in MATLAB. Rate of crack propagation has many factors governing it such as the magnitude of stress used and the stress intensity factor. There are different modes of stress as well that would result in different governing equations.

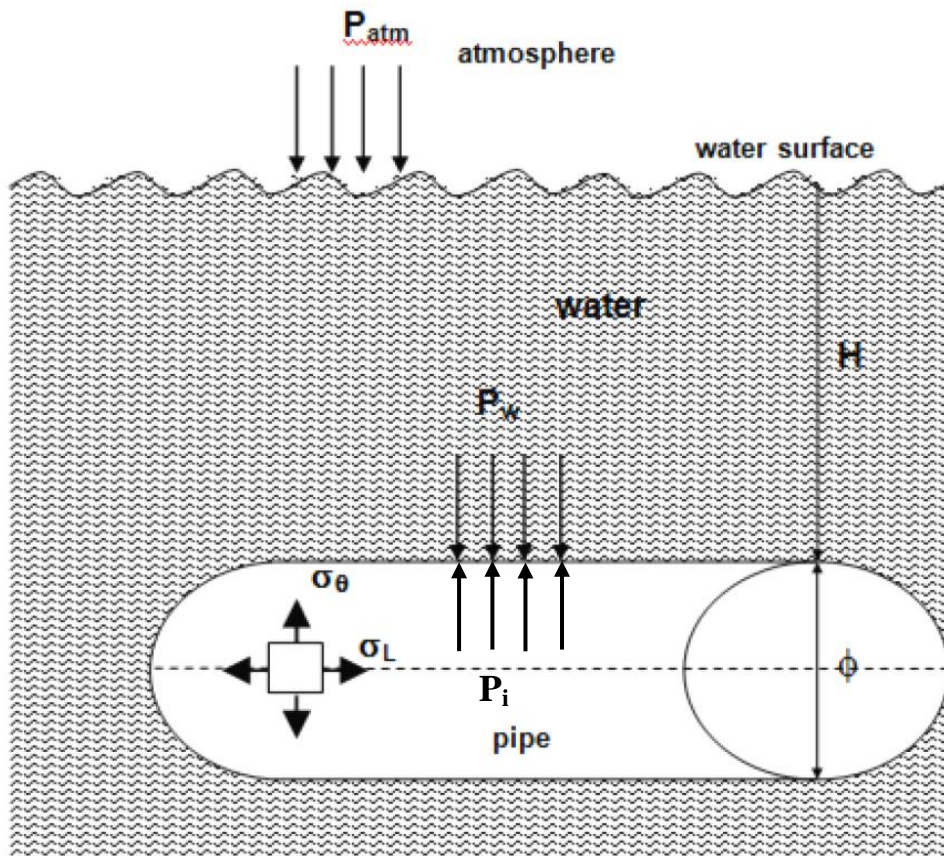


Figure 2.17: Stresses experienced by a pipe underwater[6]

Figure 2.17 shows the different types of force and stresses experienced by a pipeline underwater. It can be seen there are many parameters to consider when calculating stresses internally or externally.

Generally, when magnitude of stress is concerned, the higher the stress magnitude the faster the crack propagation will occur. This can be seen by the cumulative damage theory graph in Figure 2.4.

The sequence of stresses also plays a role in the rate of crack propagation. When applying a high load first, the residual stresses from the high load would play a part in stress calculation of the low load. Therefore in reality, having a high load first would result in a lower fatigue life compared to having a lower load first[17]. This can be seen from Figure 2.3.

Subsea pipelines are usually located deep within the surface of the sea. Subsea projects will cover shallow water (less than 300m depth), deep water (300m to 1500m depth) or Ultra deep (higher than 1500m depth). Pipelines located deeper under the sea surface are subjected to a higher pressure. This would then result in a lower RUL due to the high pressure.

CHAPTER 3 : METHODOLOGY

3.1 Introduction

The project in its entirety entails five major tasks that can be idealized or imagined as five blocks arranged sequentially, Figure 3.1. The method will first be the literature review where all previous materials related to this subject will be studied. After that, different geometries and material properties are studied before the selection is done. Once everything is in place, the model would be simulated in MATLAB. Once all the results are attained, prognosis can be carried out in order to estimate the RUL of the model.

Once the overall method is acknowledged, realization of each block is possible through detailed planning. In this regards, a suitable flowchart is developed as portrayed in Figure 3.2. The project would start with the literature review where the modes of crack as well as information regarding crack propagation are studied. It is then followed by the modeling of the system with the input of parameters such as stress distribution and stress intensity factor. Once parameters are in place, the simulation is carried out. Results are validated and repeated until accepted before the parametric study is conducted. Finally will be the report analysis and documentation of the whole project. The corresponding Gantt chart is as shown in Figure 3.3.



Figure 3.1: Methodology Flow Chart

3.1.1 Literature Review

Through the literature reviewed, all information that needs to be taken into account before the prognosis is reviewed. Parameters such as rate of crack propagation and the

relationship between stresses of different magnitudes and degradation are studied. Each crack can also be explained by different modes of stress namely Mode I, Mode II and Mode III.

3.1.2 Fundamental equation and crack propagation/model.

All fundamental equation regarding crack propagation is reviewed. The book by Budynas and Nisbett[18] is used as a big reference for the fatigue failure. A thesis by Joude[6], was supplied by the author's supervisor and also had a lot of information for the rate of crack propagation and the relationship of stresses and degradation of pipelines.

3.1.3 MATLAB modeling and computation

The strength of the project depends on this technique where computing the rate of crack growth until it reaches a critical length of a_c with all the given parameters. Certain parameters, such as the stress magnitude and crack loading should be able to be changed in order to test the rate of crack propagation in different situations.

3.1.4 Parametric Study and Regression Analysis

All parameters are analysed and a relationship between the parameters are formed. The relationship will help in simplifying the connection between the rate of crack propagation and all other parameters formed.

3.1.5 Further Analysis and Report Writing

The rate of crack propagation is further analysed under different conditions and stresses in order to see its effects until the pipeline reaches failures.

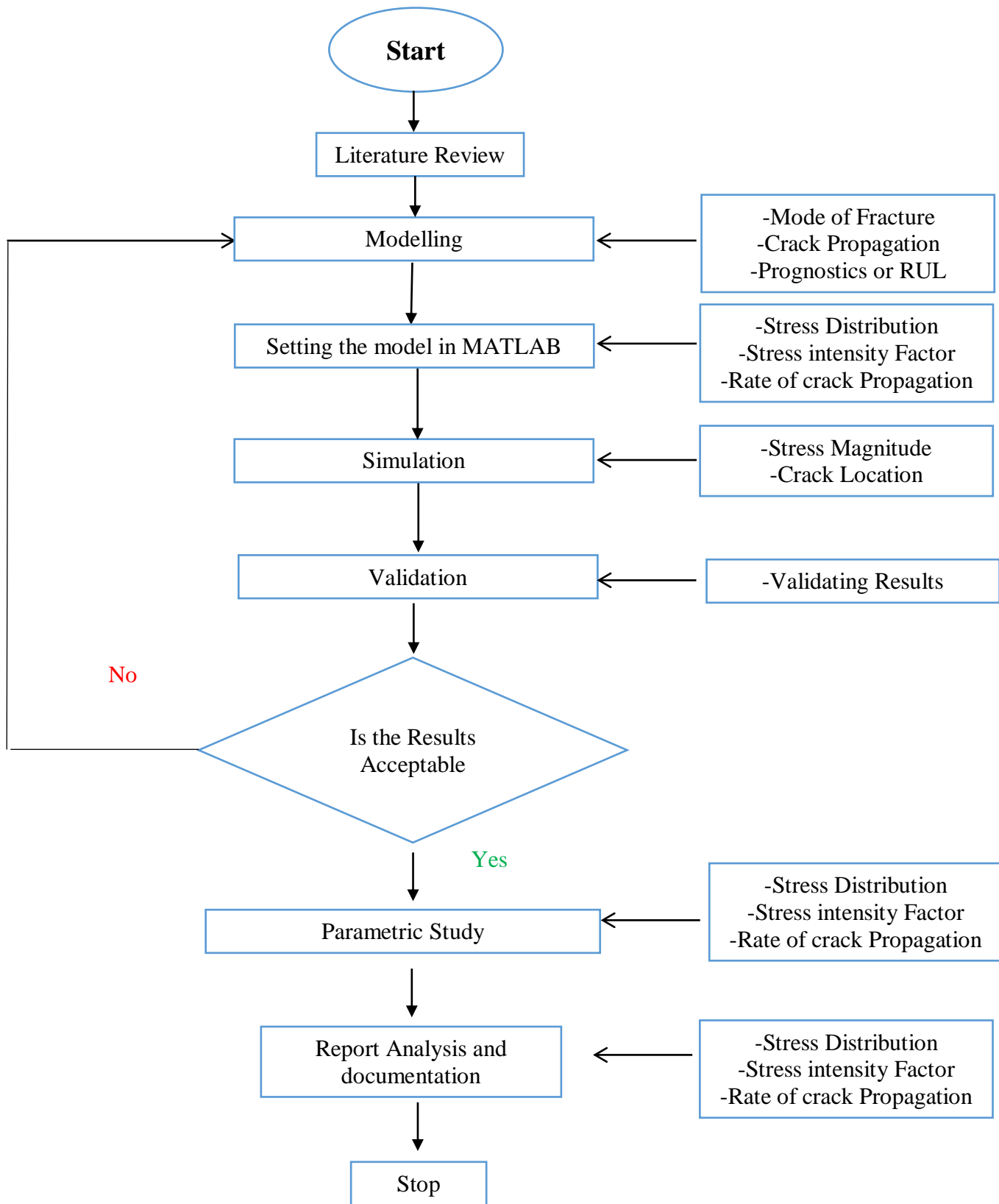


Figure 3.2: Project Flow Chart

Activities	Weeks in FYP 1													
	1	2	3	4	5	6	7	8	9	10	11	12	13	14
Modelling														
· Mode of Crack														
· Type of wall														
· Crack Location Equation														
· Setting the model in MATLAB														
Simulation														
· Simulation with Varying depths														
· Simulation with thin and thick walled pipelines														
· Simulation with internal cracks														
Parametric Study and Regression Analysis														
· Study of Simulations with Varying Magnitudes														
· Study of Simulations with thin and thick walled pipelines														
· Study of Simulations internal cracks														
Report Writing														

(a)

Activities	Weeks in FYP 2													
	1	2	3	4	5	6	7	8	9	10	11	12	13	14
Modelling														
· Mode of Crack														
· Stress Intensity Factor														
· Crack Propagation Equation														
· Setting the model in MATLAB														
Simulation														
· Simulation with Varying depths														
· Simulation with thin and thick walled pipelines														
· Simulation with internal cracks														
Parametric Study and Regression Analysis														
· Study of Simulations with Varying Magnitudes														
· Study of Simulations with thin and thick walled pipelines														
· Study of Simulations internal cracks														
Report Writing														

(b)

Milestones

NO	Milestones	Date
M1	Completion of Modelling	29/1/2016
M2	Completion of Simulation until acceptable results are obtained	19/2/2016
M3	Parametric Study and Regression analysis	25/3/2016
M4	Report Completed	8/4/2016

(c)

Figure 3.3 a) Gantt chart FYP I (b) Gant chart FYP II (c) Key Milestones

3.2 Solution Method

In order to calculate the whole crack length, the Euler's method for ordinary differential equation is used. Euler's method is one of the simplest numerical methods[19]. First of all we would make our base equation into a function. Therefore from Equation (2) we would then convert it to become:

$$\frac{da}{dN} = y(t, a) \quad (39)$$

We would then define a time step which in this case would be $dt = 1$. In Euler's Method, the crack length is calculated for each cycle by taking into account the previous crack length and adding the rate of crack length for that cycle. Finally, in order to calculate the total crack length, we can get the final equation of :

$$a_{N+1} = a_N + [y(t_N, a_N) * dt] \quad (40)$$

If a smaller time step is used however, more accurate results can be obtained. A higher number of iterations would be done in order to calculate the equation resulting in a much smaller error. However, lower step size would require a higher computational power and a much longer time needed for all simulations to be done.

CHAPTER 4 : RESULTS

4.1 Introduction

Subsea pipelines are crucial for the transportation of oil and natural gas between sites. The integrity of these pipelines has to be always kept in order to ensure that oil spills do not occur in the ocean. Prognostics of these pipelines have to be done in order to be able to foresee any risk in continuing the use of these pipelines. Besides being detrimental to the environment, these failures would also end up incurring a large cost to the user in order to fix the damage done.

Pipelines are constantly exposed to internal cyclic pressure which makes it prone to fatigue failure over time. Pipes at different locations in the subsea system will be subjected to different magnitudes of internal and external pressure. It is not only important to evaluate the magnitudes of pressure but as well as the type of crack present in the pipeline.

For this project, we will be considering longitudinal crack, semi-elliptical crack and circumferential cracks. All these cracks would then be considered at different locations with different magnitudes of stresses applied.

4.2 MATLAB Modeling

Using the MATLAB software, a code was developed for each crack type in order to calculate the crack length and the damage accumulation in the pipe. The results of each simulation are as follow.

4.2.1 Investigation of the relationship of RUL with varying magnitudes of internal pressure using longitudinal crack

For testing purposes, a MATLAB based framework was formed in order to simulate the rate of crack growth against the number of cycles done.

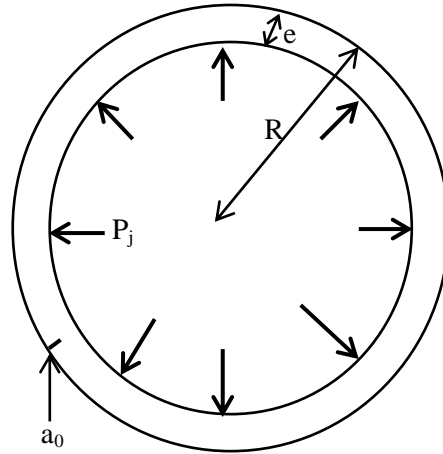


Figure 4.1: Stresses in a subsea pipeline

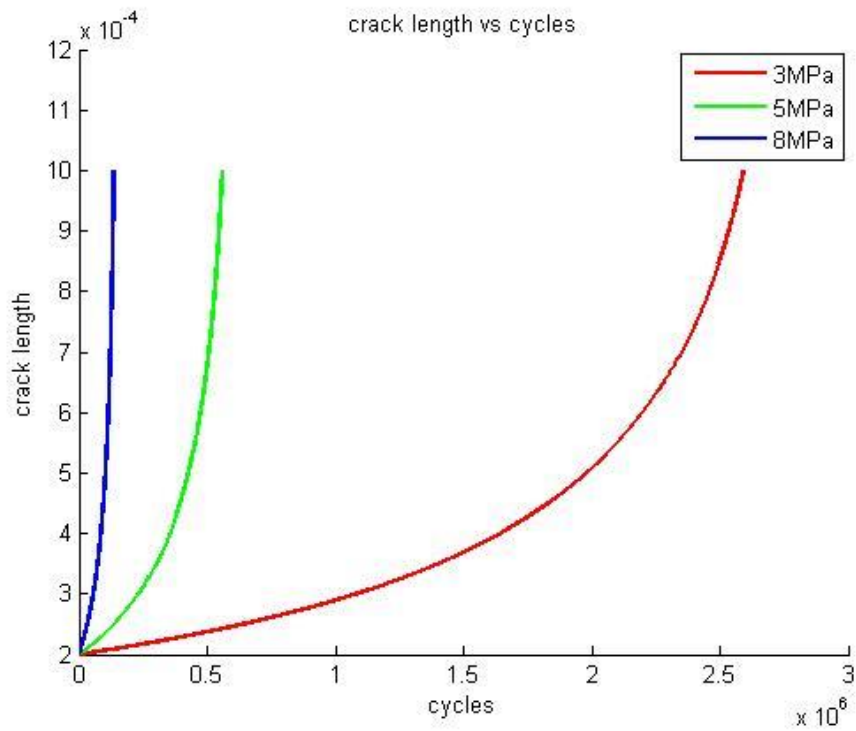
A pipe as drawn in Figure 4.1 is assumed and with the values of $R= 240\text{mm}$ and $e= 8\text{mm}$. The situation the pipe is located in will be in an offshore place having a value of $C = 2 * 10^{-11}$ with the value of $m=3$. The initial detectable crack length of $a_0 = 0.2\text{mm}$ is assumed. Then the crack lengths at different cycles are calculated using Equation (40).

Crack length is calculated until it reaches critical crack length, $a_c=e/8$ and then the calculation cycle is broken. Finally the damage accumulation is calculated using:

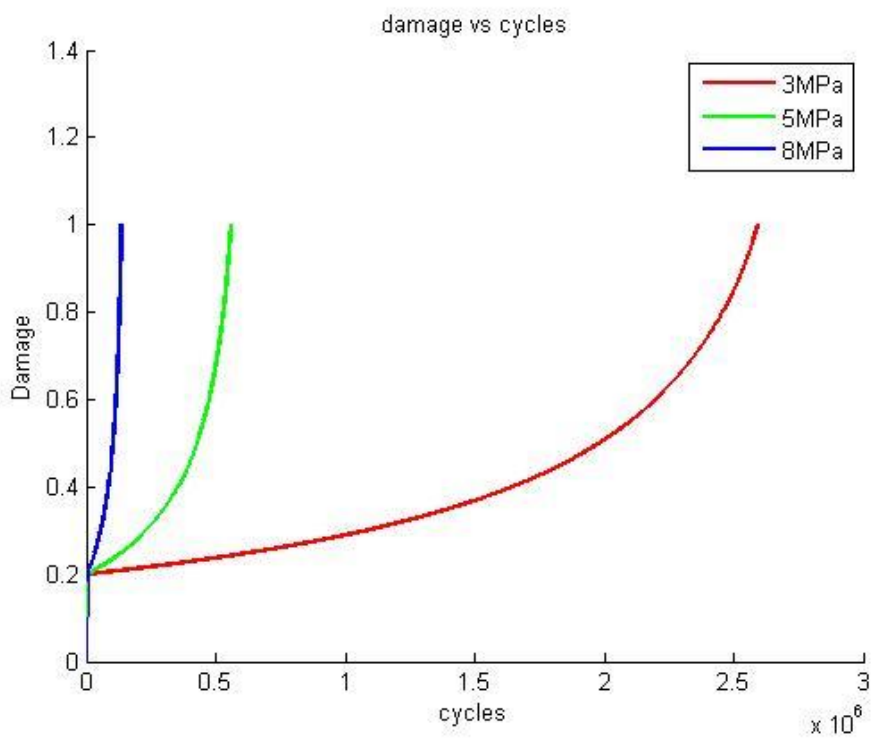
$$D_i = \frac{a_i}{a_c} \tag{41}$$

The simulation is tested using 3 different values of P_j which are 3MPa, 5MPa and 8MPa. Once all parameters are inserted into MATLAB, the whole code is simulated. The RUL can be evaluated using cycles where a higher cycle would signify a longer RUL.

The results from the simulation has come up with 2 graphs with the first one being crack length against cycles and the second one being damage accumulation against cycles.



(a)



(b)

Figure 4.2: (a) Graph of crack length against cycles for longitudinal crack (b) Graph of damage against cycles for longitudinal crack

From Figure 4.2(a), we can see that having varying magnitudes of stresses effects the number of cycles for the crack to reach its critical length. When simulating with $P_j=3\text{MPa}$, a total of 2,593,712 cycles were achieved. When using $P_j= 5\text{MPa}$, a total of 560,244 cycles were completed and finally when using $P_j= 8\text{MPa}$, only 136,781 cycles was completed before failure.

From Figure 4.2(b), we can see the difference in damage accumulation rates for all three different magnitudes of stresses. When comparing all three stresses, it can be seen that damage accumulated when using 8MPa is much faster compared to the 5MPa and 3MPa stresses. This is plotted into a graph to easily show the relationship of RUL and damage accumulation.

4.2.2 Investigation of the relationship of RUL by taking into account uncertainties in subsea pipelines

In order to simulate uncertainties in the subsea pipelines, a random value of $\pm 10\%$ of the initial crack length is used. A total of 100 different simulations were done all using a pressure value of $P_j = 8\text{MPa}$. In order to compare how the effect of uncertainties, the crack length was recorded on the 110,000 cycle for each run. The probability of each crack length was fit into a Weibull distribution curve. The results are as follows:

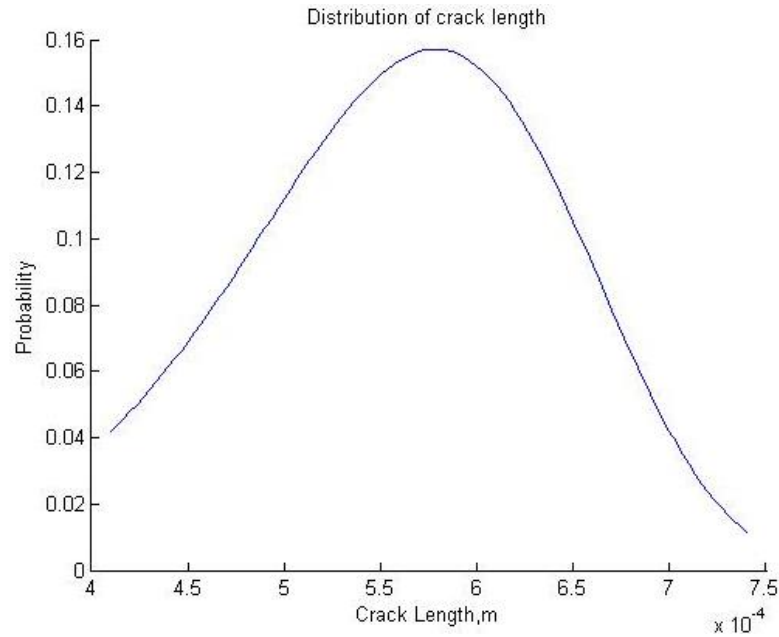
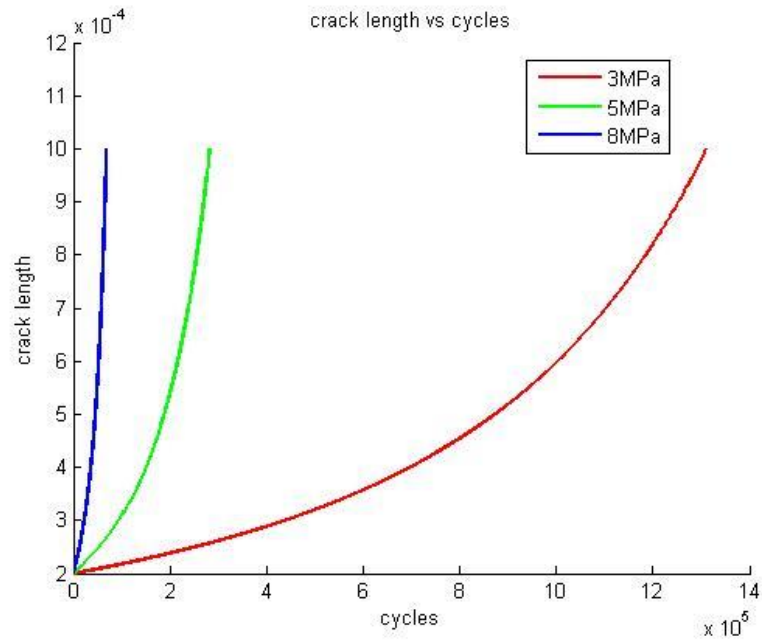


Figure 4.3: Graph of probability against crack length

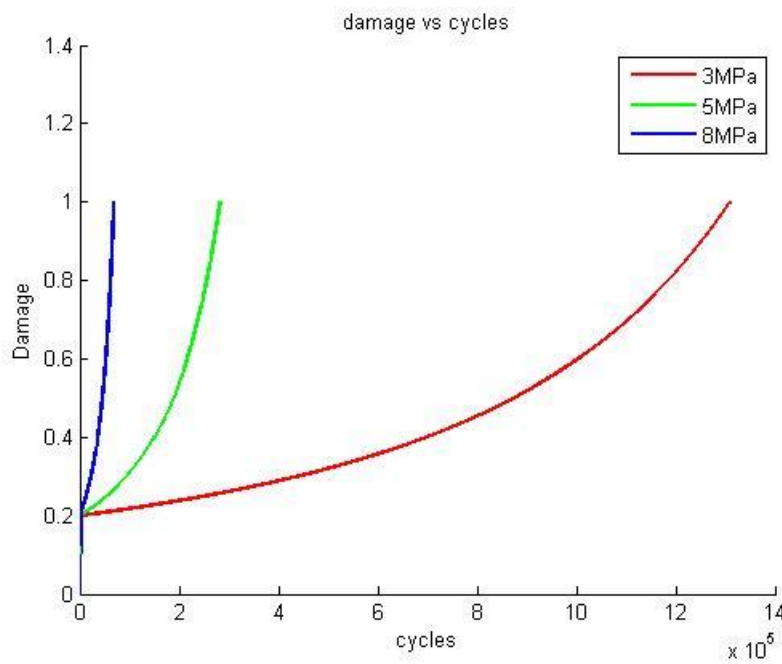
From the graph we can see that the crack length ranges from about 4.1×10^{-4} m until about 7.4×10^{-4} m. It is clear that uncertainties have such a big effect on the crack length and in turn would highly affect the RUL of the pipe as well.

4.2.3 Investigation of the relationship of RUL with varying magnitudes of internal pressure using circumferential crack

Next we will look into the circumferential crack as in Figure 2.11. When modeling this problem, the same parameters as in the previous section were used for easy comparison. However the stress intensity factor as in Equation (21) together with Equation (22-24) is used for circumferential crack. The results are as follows:



(a)



(b)

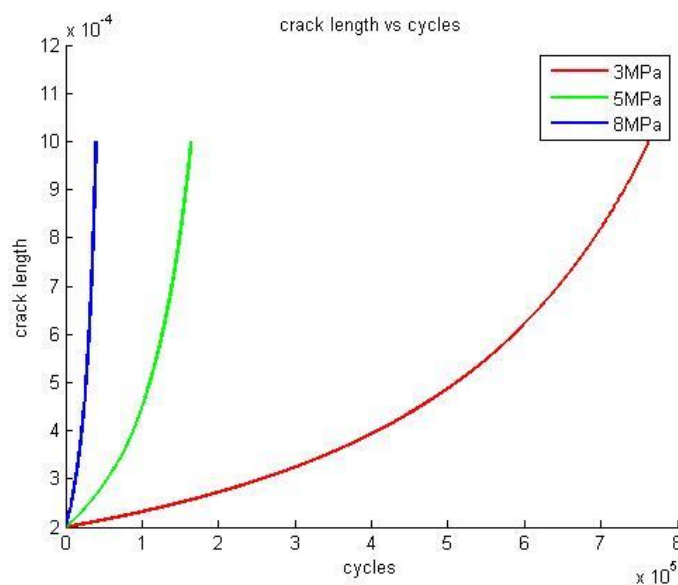
Figure 4.4: (a) Graph of crack length against cycles for circumferential crack (b) Graph of damage against cycles for circumferential crack

We can see from the graph that the trend of crack propagation is similar in which the rate of crack propagation is highly affected by the magnitude of force used. When a pressure value of $P_j = 3\text{MPa}$ is used, a total of 1,309,723 cycles were completed before failure occurred. Similarly when using $P_j = 5\text{MPa}$, a total of 282,902 cycles were completed and finally using, $P_j = 8\text{MPa}$ resulted in a total of 69,070.

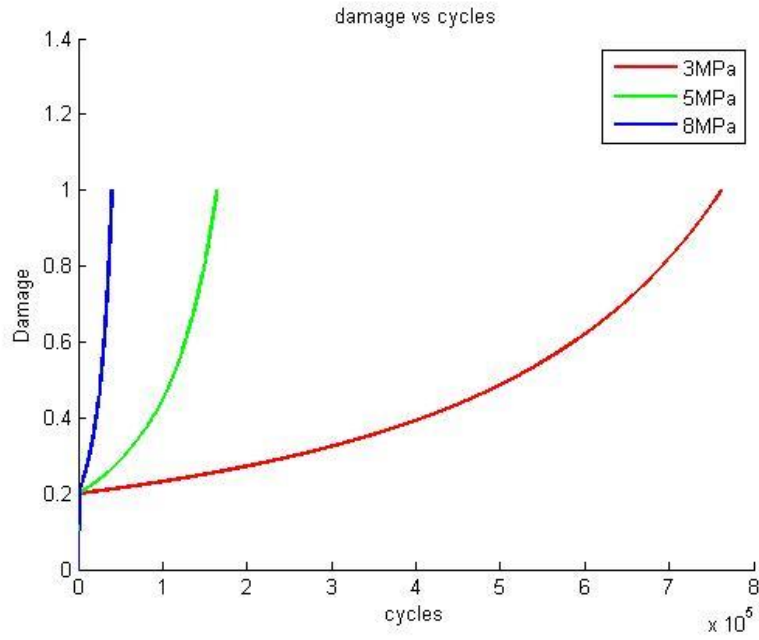
Based on Figure 4.4, we can conclude that the magnitude of stress highly affects the damage accumulation rate. When a higher magnitude of stress is used, the damage accumulation occurs at a faster rate causing the pipe to fail at a much shorter time.

4.2.4 Investigation of the relationship of RUL with varying magnitudes of internal pressure using semi-elliptical crack

Semi-elliptical crack can occur as shown in Figure 2.10. Modelling this problem is done using the same parameters as previous problems. However for semi-elliptical crack the crack length, c and crack depth, a are taken into account. For this problem, we use an a/c ratio of 0.2. The rate of crack propagation is simulated and plotted into a graph using MATLAB. The results are as follows:



(a)



(b)

Figure 4.5: (a) Graph of crack length against cycles for Semi-elliptical crack (b) Graph of damage against cycles for Semi-elliptical crack

We can see from the graph that the trend of crack propagation when taking into account a semi-elliptical crack is also similar in which the rate of crack propagation is highly affected by the magnitude of force used. When a pressure value of $P_j = 3\text{MPa}$ is used, a total of 762,310 cycles were completed before failure occurred. Similarly when using $P_j = 5\text{MPa}$, a total of 164,661 cycles were completed and finally using, $P_j = 8\text{MPa}$ resulted in a total of 40,203.

From the graph, we can see that the damage accumulation is directly proportional to the magnitude of stress exerted on the pipe. When a higher stress is used, the damage accumulates at a much faster rate, causing the pipe to reach failure within a shorter time.

4.2.5 Comparing the relationship of RUL with varying types of cracks

In order to compare all 3 different types of curves, the 3 MPa line for each crack was extracted and placed on the same graph.

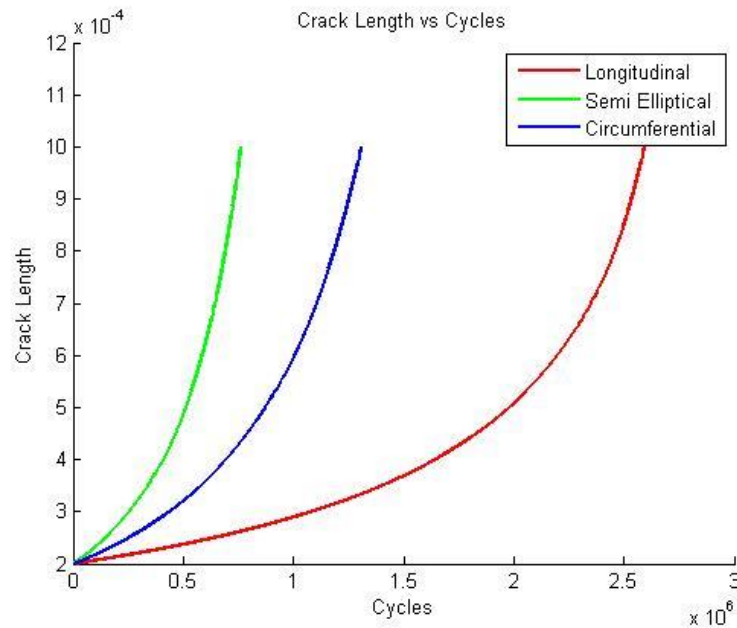


Figure 4.6: Comparison of 3 graphs

From Figure 4.6, we can see that the semi elliptical crack would be the most dangerous crack among the three cracks. This is then followed by the circumferential crack and then the longitudinal crack. However, the trend of crack propagation is the same among the different types of cracks. This makes the comparison of cracks very easy when put side by side.

4.3 Discussion

Based on the results from the simulation, there are a few conclusions that can be come up with. First of all, we can conclude a proper relationship between the magnitudes of stresses with the rate of crack expansion of the pipes. When a higher stress is used, the rate of crack propagation becomes much faster. This can be explained by the increase in stress intensity factor. Thus, we can conclude that the higher the stress exerted onto the pipe, the lower the RUL of pipe.

When talking about the types of crack in the pipe, we compare longitudinal, circumferential and semi-elliptical crack. We use a stress of 3MPa to standardize the parameters when comparing. For longitudinal crack, a total of 2,593,712 cycles were

completed before failure. For circumferential crack, a total of 1,309,723 cycles were completed before failure, and lastly, for semi-elliptical crack, a total of 2.212,193 cycles were completed.

Lastly, when taking into consideration uncertainties in the initial crack length, we can see that the crack growth varies very differently. This is dangerous as the estimation of initial crack length might be slightly wrong causing the pipe to fail much faster.

From the results, we can conclude that knowing the type of crack is very crucial in calculation the RUL of pipes. For example, when subjected to 3 MPa, circumferential crack fails almost twice as fast as the longitudinal crack. A small mistake in identifying the type of crack present may end up causing unforeseen failures.

CHAPTER 5 : CONCLUSION AND RECOMMENDATION

5.1 Conclusion

Throughout the duration of this project, the whole concept of fatigue failure was learnt. All literature obtained was helpful in order to complete this whole project. The results obtained from this project follow the trend as all other crack propagation models. Some important conclusions are as follows:

- Remaining useful life is very much affected by the stresses acting on the pipe. For a noticeable crack length of a_0 the higher stress exerted the faster the crack would reach its critical length a_c .
- An accurate estimation of the RUL can be calculated from the conditions and parameters based on the type and orientation of the crack.
- Comparison between a longitudinal crack, circumferential crack and semi-circular is done.
- Further analysis on the rate of crack propagation based on computations done in MATLAB.

5.2 Recommendation

This project can be further expanded as there are a lot of other parameters that can be considered when doing analysis of RUL. Rotational force was not considered in the calculations of crack propagation as well other types of cracks such as external crack, thumbnail crack and many others. The stress intensity formula for each crack can be obtained through research. Also, the average pressure inside pipelines was not considered. Adding this into the equation will definitely change the results slightly. Mode II and Mode III of fracture was not touched as well. These two modes would result in a different stress intensity factor compared to the Mode I fracture currently being studied. Finally, a stochastic analysis approach can also be done instead of deterministic. Expanding the MATLAB software will allow a much wider range of analysis to be carried out with ease. Lastly, during the operation of the pipeline, temperature and pressure would play a role in changing the rate of crack propagation. Another parameter that can be taken into account would be the frequency of load applied.

REFERENCES

- [1] F. Adams, "The Book Of Prognostics," *The Internet Classics Archive*, 2009.
- [2] NOAA, "Types of Offshore Oil and Gas Structures," *Office of Ocean Exploration and Research*, vol. http://oceanexplorer.noaa.gov/explorations/06mexico/background/oil/media/types_600.html, 2008.
- [3] P. Vaidya, "Prognosis- Subsea Oil and Gas industry," *Annual Conference of the Prognostics and Health Management Society*, 2010.
- [4] C. T. Sun and Z.-H. Jin, "Fracture Mechanics," 2012.
- [5] K. El-Tawil and A. A. Jaoude, "Stochastic and nonlinear-based prognostic model," *Systems Science & Control Engineering*, vol. 1, pp. 66-81, 2013.
- [6] A. Jaoude, "Advanced Analytical Model for the Prognostic of Industrial Systems Subject to Fatigue," 2013.
- [7] J. Schijve, "Fatigue of structures and materials in the 20th century and the state of the art," *International Journal of Fatigue*, vol. 25, pp. 679-702, 2003.
- [8] J. Yan, "crack propagation rate 28Jan2016," 2015.
- [9] N. H. Dao and H. Sellami, "Stress intensity factors and fatigue growth of a surface crack in a drill pipe during rotary drilling operation," *Engineering Fracture Mechanics*, vol. 96, pp. 626-640, 2012.
- [10] K. K. Jefferson, "Fracture," *Virginia Tech Materials and Engineering* . Obtained from http://www.sv.vt.edu/classes/MSE2094_NoteBook/97ClassProj/anal/kim/intensity.html 2000.
- [11] J. A. Collins, *Failure of Materials in Mechanical Design: Analysis, Prediction, Prevention*: Wiley, 1993.
- [12] R. G. F. Ivatury S. Raju, Sambu R.Mettu, "Stress Intensity Factors for Part-Through Surface Cracks in Hollow Cylinders," *Research Gate*, August 1992.
- [13] A. J. McEvily and J. Kasivitanuay, *Metal Failures: Mechanisms, Analysis, Prevention*: Wiley, 2013.

- [14] MyDatabook.org, "Stress for Thick Walled Cylinders using Lamé's Equations," *Obtained from <http://www.mydatabook.org/solid-mechanics/stress-for-thick-walled-cylinders-and-spheres-using-lames-equations/>*, 2015.
- [15] eFunda, "Thin-walled pressure vessels," *Obtained from http://www.efunda.com/formulae/solid_mechanics/mat_mechanics/pressure_vessel.cfm*, 2015.
- [16] I. Vasovic, S. Maksimovic, K. Maksimovic, S. Stupar, G. Bakic, and M. Maksimovic, "Determination of Stress Intensity Factors in Low Pressure Turbine Rotor Discs," *Mathematical Problems in Engineering*, 2014.
- [17] eFatigue, "Fatigue from variable amplitude loading," *Obtained from https://www.efatigue.com/training/Chapter_9.pdf*, 2015.
- [18] R. G. Budynas and J. K. Nisbett, "Shingleys Mechanical Engineering Design," Ninth Edition.
- [19] J. F. Epperson, *An Introduction to Numerical Methods and Analysis*: Wiley, 2013.
- [20] L. Y. A. Fatemi, "Cumulative fatigue damage and life prediction theories: a survey of the state of the art for homogeneous materials," *PII: 80142-1123(97)00081-9*.

APPENDIX-A

I) Summary of the literature review of pipe prognostics

Author/Year	Objective	Method/case problem	Remark
El-Tawil and Jaoude (2013)	Developed analytical prognostic model base on non-linear damage laws	stochastic approach	Finding a link between prognostics and reliability
Vaidya (2010)	Highlight limitation of classical approach and the need for Bayesian approach	Explain Technical health and factors influencing RUL	Bayesian network used widely nuclear and avionics field
Budynas, Nisbett	To study fatigue failure under variable loadings	All basic concepts regarding crack propagation and fatigue life are explained	Very informative as a start to learn the rate of propagation concept
Jaoude (2013)	To study both linear and non-linear damage laws	Stochastic approach	Developed a prognostic model based on linear and non-linear laws

Table A-1: Summary of cumulative fatigue damage theories: work before 1970[20]

Year	Developer Name	Model	Physical basis	Equation
1945	Miner	Miner LDR	Constant energy absorption per-cycle	$D = \frac{\sum n_i}{N_i}$
1949	Machlin	Machlin Theory (metallurgic LDR)	Constant dislocation generation per-cycle	$D = \sum n_i \int_0^{P/2} R_{gi} dt$
1952	Shanley	Shanley Theory	Crack growth, crack length as damage measure	$D = \sum \left(\frac{a_0}{a_c}\right)^{1-r_i}$
1954	Marco & Starkey	Marco-Starkey theory	Conceptual	$D = \sum r_{ix_i}, x_i > 1$
1955	Henry	Henry Theory	Endurance limit change	$D = \frac{\sigma_{co} - \sigma_c}{\sigma_{co}} = \sum \frac{r_i}{1 + (1 - r_i)/\lambda_i}$
1956	Coffin	Strain version of LDR	Directly converted from stress version	$D = \frac{\sum n_i (\Delta \epsilon_p)_i^{1/\alpha}}{C^{1/\alpha}}$
1956	Corten & Dolon	Corten-Dolon model	Number of damage nuclei	$D = \sum m_i p_i n_{bi}$
1959	Frudenthal and Heller	Frudenthal-Heller theory	Fictitious life curve, probabilistic analysis	$D = \sum \left(\frac{n_i \omega_i}{N_i}\right)$
1960	Grover	Grover's two-stage damage theory	Crack initiation and crack propagation, two-stage linear evolution	Initiation: $\sum \frac{n_i}{\alpha_i N_i} = 1$ Propagation: $\sum \frac{m_i}{(1-\alpha_i) N_i} = 1$

1961	Gatts	Gatts theory	Endurance limit change	$\gamma_c = \frac{\sigma_c}{\sigma_{co}} = \gamma_a \left[1 - \frac{1}{\frac{\gamma_u}{\gamma_u - 1} r + \frac{\gamma_a}{\gamma_a - 1} (1 - r)} \right]$
1961	Bluhm	Bluhm's hypothesis	Endurance limit change	$d_n = \gamma_{(n)} - \gamma_{e(n-1)} $
1961	Valluri	Valluri theory	Crack growth and dislocation, fracture mechanics	$\frac{da}{dN} = Cf(\sigma)a$
1966	Scharton and Crandall	Scharton-Crandall theory	Crack growth fracture mechanics	$\frac{da}{dN} = a^{m+1}f(\sigma_{ij})$
1966 1967	Manson et al.	Double linear damage rule (DLDR)	Crack initiation and crack propagation, two-stage linear evolution (EMP)	Phase 1: $\sum \frac{n_i}{N_{1,i}} = \sum \frac{n_i}{N_f - PN_f^{0.6}} = 1$ Phase 2: $\sum \frac{m_i}{N_{II,i}} = \sum \frac{m_i}{PN_f^{0.6}} = 1$

TABLE A-2: Summary of cumulative fatigue damage theories: DCA, refined DLDR and DDCA

Year	Developer Name	Model	Physical basis	Equation
1981	Manson & Halford	Damage curve approach	Effective microcrack growth	$D = \sum r_{iq}$ where $q = (N_i N_r)^\beta$, $\beta = 0.4$
1981	Manson and Halford	Damage Refined DLDR	Based on DCA and linearization	$D_I = \sum \left(\frac{n_I}{N_I}\right)_i N_I = N - N_{II} B = 0.65$ $D_{II} = \sum \left(\frac{n_{II}}{N_{II}}\right)_i N_{II} = B N \left(\frac{N_r}{N}\right)^\alpha \alpha = 0.25$
1986	Manson and Halford	Double damage curve approach (DDCA)	Based on both DCA and refined DLDR	$D = \sum [(pr_i)_k + (1 - p_k)r_{kq}]^{\frac{1}{k}}$ $A = .35, k = 5$ $p = \frac{A \left(\frac{N_r}{N_i}\right)^\alpha}{\left[1 - B \left(\frac{N_r}{N_i}\right)^\alpha\right]}$ $B = 0.65, \alpha = 0.25, \beta = 0.4$

TABLE A-3: Summary of cumulative fatigue damage theories: hybrid theories

Year	Developer Name	Model	Physical basis	Equation
1971	Bui-Quoc et al.	Stress version	Hybridization, endurance limit change	$D = \frac{1 - \gamma_e}{1 - \gamma_{ec}} = \sum \frac{r_i}{r_i + (1 - r_i) \frac{\gamma_i - (\frac{\gamma_i}{\gamma_u})^m}{\gamma_i - 1}}$ $m = 8$
1971	Bui-Quoc et al.	Strain Version	Transplanted from the stress version	$D = \frac{1 - \lambda_e}{1 - \lambda_{ec}} = \sum \frac{r_i}{r_i + (1 - r_i) \frac{\lambda_i - (\frac{\lambda_i}{\lambda_f})^m}{\lambda_i - 1}}$ $m = 8$
1981	Bui-Quoc	Fictitious load modification	Endurance limit change, to account for load interaction effects	$D = \sum \frac{r_i}{r_i + (1 - r_i) \frac{\lambda_i' - (\frac{\lambda_i'}{\lambda_f})^m}{\lambda_i' - 1}}$ $m = 8$
1982	Bui-Quoc	Cycle-ration modification	Endurance limit change, to account for load interaction effects	$D = \sum \frac{r_{iv}}{r_{iv} + (1 - r_{iv}) \frac{\lambda_i - (\frac{\lambda_i}{\lambda_f})^m}{\lambda_i - 1}}$ $m = 8$

TABLE A-4: Summary of cumulative fatigue damage theories: recent theories based on crack growth

Year	Developer Name	Model	Physical basis	Equation
1977	Miller & Zachariah	Double exponential law (1 st version)	Two-stage crack growth	$N_{I,l} = N_{f,1} \left(\frac{r_1 + r_2 - 1}{r_2} \right)$
1980 1981	Ibrahim & Miller	Double exponential law (2 nd version)	Two-stage crack growth	$r_2 = (1 - r_1) \left(\frac{1}{1 - r_{I,1}} \right) \ln \frac{\left(\frac{a_{I,1}}{a_f} \right)}{\ln \left(\frac{a_0}{a_f} \right)}$ $D = \frac{a}{a_f} = \left(\frac{a_I}{a_f} \right)^{(1-r)/(1-r_I)}$
1982	Miller	Short Crack theory	MSC,PSC,E-P fracture mechanics	$\frac{da}{dN} = A(\Delta\gamma)^\alpha (d - a)$ for MSCs: $a_0 \leq a \leq a_t$ $\frac{da}{dN} = B(\Delta\gamma)^\beta a - C$ for PSCs: $a_t \leq a \leq a_f$
1989	Ma & Laird	Ma-Laird theory	Crack population	$D = \sum \frac{P_i}{P_{crit}}$ $= K \sum n_i \left[(\Delta\gamma_p/2)_i \alpha_i - \left(\frac{\Delta\gamma_p}{2} \right)_{limit} \right]$

1991	Vasek & Polak	Vasek-Polak model	Microcrack kinetics equivalent crack length	Initiation: $D = 2D_c r$ $D \leq r \leq \frac{1}{2}$ Propagation: $D = D_c + \frac{D_c}{m} [e^{m(2r-)} - 1]$ $1/2 \leq r \leq 1$
------	---------------	-------------------	--	---

TABLE A-5: Summary of cumulative fatigue damage theories: models based on modifying life-curve

Year	Developer Name	Model	Physical basis	Equation
1976	Subramanyan	Subramanyan model	Convergence to the knee-point	$r_i = 1 - \left\{ r_{i-1} + \left[r_{i-2} + \dots + (r_2 + r_1^\alpha)^\alpha \dots \right]_{i-2}^\alpha \right\} a h a_{i-1}$
1978	Hashin & Rotem	Hashin-Rotem theory	Two types of convergence	Formulation based on static strength point, and formulation based on endurance limit point
1985	Leipholz	Leipholz's approach	Experimental determination	Modified life curve is obtained from repeated multi-level block tests
1990	Ben-Amoz	Bound theory	Upper and lower bounds of convergence lines	Bounds formed by Miner rule and Subramanyan model; bounds formed by DLDR and Subramanyan model; and statistical bounds

TABLE A-6: Summary of cumulative fatigue damage theories: energy-based damage theories

Year	Developer Name	Model	Physical basis	Equation
1973	Bui-Quoc	Bui-Quoc model	Constant total plastic energy at failure	$W_f = \sum n_i \Delta W_i$ $= \frac{2K'M_{n'+1}}{n'+1} \sum r_i N_{fi}^{1-c(n'+1)}$
1978	Radhakrishnan	Radhakrishnan approach	Crack growth rate is related to plastic energy	$r_m = 1 - \sum_{i=1}^{m-1} \frac{W_{fi}}{W_{fm}} r_i$
1984	Kujowski and Ellyin	Plastic strain energy(hysteresis energy)	Convergence plastic strain energy	In the plastic strain energy vs life diagram, isodamage curves converge to the apparent fatigue limit, rather than to the original limit
1984	Kliman	Kliman Theory	Block spectrum, similar basis to the above	$D_b = \frac{W_b}{W_{fR}} = \frac{1}{W_{fR}} \sum \Delta W_i n_{bi}$
1987	Golos and Ellyin	Total strain energy	Convergence total strain energy	In the total strain energy vs life diagram, isodamage curves converge to the apparent fatigue limit, rather than to the original limit
1987	Niu et al.	Niu Theory	Strain hardening and plastic strain energy	$D = \phi^{1/[(n'+\alpha)(1+\beta)]} = \sum r_i^{1/(n'+\alpha)}$
1988	Leis	Leis model	Related to two exponents in strain-life equation	$D = \frac{4\sigma'_f}{E} (2N_f)^{2b_1} + 4\sigma'_f \epsilon'_f (2N_f)^{b_1+c_1}$

TABLE A-7: Summary of cumulative fatigue damage theories: continuum damage mechanics approaches

Year	Developer Name	Model	Physical basis	Equation
1974	Chaboche	Chaboche model	Based on effective stress concept in CDM. Only differing in number of variables assumed in the damage rate equation and boundary conditions	$D = 1 - [1 - r^{1/(1-\alpha)}]^{1/(1+\beta)}$
1979	Lemaitre & Plumtree	Lemaitre-Plumtree model		$D = 1 - (1 - r)^{\frac{1}{1+p}}$
1989	Li et al.	Li-Qian-Li model	Besides above, dislocation variable is involved	$D = 1 - \left(\frac{\lambda_i}{\lambda_0}\right)_p$
1990	Wang & Lou	Wang-Lou model	Based on effective stress concept in CDM. Only differing in number of variables assumed in the damage rate equation and boundary conditions	$D = D_c - (D_c - D_0)(1 - r)^{1-\beta}$
1990	Lemaitre & Chaboche	Lemaitre-Chaboche model		$D = \sum r_i^{1/(1-\alpha)}$
1991	Chow & Wei	Three-dimensional CDM model	CDM approach in three-dimensional space	A damage effective tensor was introduced and a generalized three-dimensional isotropic CDM model was proposed based on effective stress concept

1992	Wang	Wang model	Based on effective stress concept in CDM. Only differing in number of variables assumed in the damage rate equation and boundary conditions	$D = 1 - (1 - r)^{1/[1+n(R)]}$
------	------	------------	---	--------------------------------

TABLE A-8: Summary of cumulative fatigue damage theories: other approaches

Year	Developer Name	Model	Physical basis	Equation
1973	Landgraf	Landgraf model	Strain version of LDR involving mean stress	$\frac{D}{reversal} = \frac{1}{2N_f}$ $= \left[\frac{\sigma'_f - \sigma_m}{\epsilon'_f E} \left(\frac{\Delta \epsilon_p}{\Delta \epsilon_e} + \frac{\sigma_m}{\sigma'_f} \right) \right]_{1/(b-c)}$
1974	Kramer	Surface layer stress approach	Surface layer stress change	$D = \sum \left(\frac{\sigma_{si}}{\sigma_s^*} \right)$
1982	Fong	Fong Theory	Assuming a linear damage rate	$D = \sum (e_{kr_i} - 1) / (e_k - 1)$ $k \neq 0$
1982	Buch et al.	A correction approach	Using correction factor C	$N'' = N_{cal}'' \left(\frac{N_{exp}'}{N_{cal}'} \right) = N_{cal}'' C$

1984	Azarai et al.	Plastic strain evolution model	Plastic strain evolution and accumulation	$D = \sum \left(\frac{\Delta \epsilon_p - \Delta \epsilon_{po}}{\Delta \epsilon_{pf} - \Delta \epsilon_{po}} \right)_{1-1/c}$
1984	Kurath et al.	Plastic work based damage model	Plastic work, LDR, load interaction	$D_b = \sum_{i=1}^k \frac{2n_i}{(2N_f)_i} \left(\frac{\Delta \sigma_i}{\Delta \sigma_h} \right)_{1/d}$
1987	Inoue et al.	Micro-damage mechanics model	Involving PSB parameter	$D(\vec{N}, n) = \left[\frac{\vec{N}}{\frac{1}{2}} * \frac{\vec{N}}{\frac{1}{2}} * (\vec{N})_{max} \right] \left(\frac{n}{N_f} \right)_{-ck/m}$
1988	Cordero et al.	PSB version of LDR	Persistent slip band density	$\sum \left(\frac{n_i}{N_{fi}} \right) = DS = 1 + D_2/D_1$
1989	Ikai et al.	ES-Miner rule	Internal stress and effective stress evolutions	Applied stress can be resolved into internal and effective stresses. The internal stress is representative of the fatigue resistance of a material while the effective stress is responsible for the fatigue damage.
1989	Abuolfoutouh & Halford	A model based on resistce-to-flow	Change in resisitance-to-flow	$\frac{dX}{dN} = \pm J_{2+b} e^{(cX+d)}$
1990	Topper et al.	Overload damage model	Crack opening and closure	$D = \sum D_{o1} + \sum D_{ss} + \sum D_{int}$
1992	Pasic	Unified approach	CDM and fracture mechanics	This is an approach combining fracture mechanics with damage mechanics